

# A study of dependence of Zn–Ni codeposition in acetate–chloride electrolyte on alloy deposition conditions

A. Petrauskas,  
L. Grincevièienë,  
A. Èeðùnienë,  
V. Jasulaitienë

*Institute of Chemistry A. Goštauto 9,  
LT-01108 Vilnius, Lithuania*

Codeposition of Zn–Ni in acetate–chloride electrolyte has been investigated as a function of current density ( $i_c$ ), temperature of plating solution and thickness of deposits by using the potentiodynamic stripping method. The quantity of free Ni in Zn–Ni alloys was found to increase with an increase in the temperature of the plating solution. The quantity of free Ni in coatings of the same thickness deposited in acetate–chloride electrolyte at 50 °C increased with a decrease in  $i_c$ . Their phase composition changed with an increase in coating thickness.

**Key words:** electrodeposition, 50 °C Zn–Ni coatings, acetate–chloride electrolyte, stripping

## INTRODUCTION

Studies of Zn–Ni codeposition can be divided into two parts: investigation of regularities of both normal and anomalous Zn–Ni codeposition and determination of phase composition of Zn–Ni alloys. During the research of reasons for normal and anomalous Zn–Ni codeposition it has been determined that they are conditioned by  $i_c$  [1], the magnitude of the deposition potential ( $E_c$ ) [2, 3], the  $[\text{Zn}^{+2}] / [\text{Ni}^{+2}]$  ratio [4] in the electrolyte and by the temperature.

Studies of the phase composition of Zn–Ni alloys were performed by the XRD and the potentiodynamic stripping methods [4–12]. The latter is a classic method. Sometimes these methods are merged. By using the potentiodynamic stripping method it has been determined that four anodic current ( $i_a$ ) peaks A, B, C and D emerge in potentiodynamic curves (PDC) [7–9, 11]. These  $i_a$  peaks are attributed to Zn dissolution from certain phases of Zn–Ni alloy. The  $i_a$  peak A being in the most negative range of potentials corresponds to Zn anodic dissolution from the  $\eta$ -phase. This phase represents a solid 1% Ni solution in Zn. The  $i_a$  peak B is attributed to Zn dissolution from the  $\alpha$ -phase. It is Zn solution in Ni of a varying composition. The composition of this phase can vary in a wide range of Zn concentration up to 30% Zn solution in Ni. The  $i_a$  peak C is attributed to Zn dissolution from the  $\gamma$ -phase ( $\text{Ni}_5\text{Zn}_{35}$ ), while the  $i_a$  peak D is attributed to the anodic dissolution of active porous Ni. The opinions concerning the processes occurring in the  $i_a$  peak D differ [13].

White Zn–Ni alloys are electrodeposited at temperatures 20 °C to 30 °C. Therefore, most of the studies were performed in this temperature range and only a few works were done at 50 °C [4, 14, 15]. The mechanism of electrolytic Zn–Ni alloy deposition has been studied in sulphate, chloride and sulphate–chloride electrolytes with ammonia ions. The works devoted to Zn–Ni alloy deposition in ammonia ion free acetate electrolytes are few in number [4–16]. Ammonia ions complicate treatment of wastewater in industry; therefore, they should be removed from plating solutions. Furthermore, it has been shown that black Zn–Ni alloy of good quality can be deposited from acetate–chloride electrolyte [15].

The aim of the present work was to determine the dependence of Zn–Ni codeposition in acetate–chloride electrolyte on deposition conditions.

## EXPERIMENTAL

Potentiodynamic studies were performed with a PI 50-1 potentiostat in an ISE-2 thermostatic electrochemical cell on a Pt electrode with an area of 1 cm<sup>2</sup>. Nickel foil was used as the anode. The anode was separated from the cathode by a diaphragm. The electrolyte was agitated neither during deposition nor potentiodynamic stripping. To prepare solutions the following salts were used:  $\text{Ni}(\text{CH}_3\text{COO})_2 \cdot 4\text{H}_2\text{O}$ ;  $\text{ZnCl}_2$ ;  $\text{KCl}$ ;  $\text{CH}_3\text{COOH}$ ;  $\text{H}_3\text{BO}_3$ . All the used reagents were at least of *pro analysis* grade.

A plating solution of the following composition was used in all experiments (mol l<sup>-1</sup>):  $\text{Ni}(\text{CH}_3\text{COO})_2$

· 4H<sub>2</sub>O – 0.56; KCl – 0.91; H<sub>3</sub>BO<sub>3</sub> – 0.5 with various concentrations of ZnCl<sub>2</sub>.

10% and 50% solutions of ZnCl<sub>2</sub> were prepared dissolving the whole prepacked bag of precise weight in bidistilled water. Then the required quantity was added to the mentioned above plating solution, and the excess of H<sub>2</sub>O was evaporated. The Pt electrode was chosen as an alternative to the Fe electrode, which during potentiodynamic stripping began to dissolve and *i<sub>a</sub>* peaks emerged in PDC. The pH of all electrolytes was equal to 5.0. Potentiodynamic stripping was performed in plating solution. All the potential values are given with respect to the Ag/AgCl/KCl<sub>sat</sub> reference electrode.

To determine *CE*, every Zn–Ni alloy specimen was weighed and the percentage of Zn and Ni in the alloy was determined by means of electron probe microanalysis with a JXA-50A (JEOL) microanalyser. The quantity of Zn–Ni alloy to be deposited (*g*) after a certain electric charge (*Q*) had been passed through electrolyte was calculated from the analysis data. In order to deposit coatings of the same thickness, the alloy deposition time was chosen depending on alloy deposition *CE*. With this in mind, primarily an approximate *CE* was determined, following which it was refined while depositing a new alloy coating of the same thickness:

$$MT = Q(X_{Ni} 0.304 + X_{Zn} 0.339), CE = \frac{M_E}{M_T} 100(\%),$$

where: *M<sub>T</sub>* is the calculated alloy mass (*g*) to be deposited after a certain *Q* (*C*) was passed; *M<sub>E</sub>* is the experimentally determined alloy mass (*g*) after a certain *Q* was passed; *X<sub>Ni</sub>* and *X<sub>Zn</sub>* are weight portions in the alloy.

XPS compositions of Zn–Ni coatings were obtained using an ESCALAB MKII spectrometer (VG Scientific, Great Britain, radiation MgK<sub>α</sub> – 1253.6 eV, capacity 300 W). The photoelectron spectra of Ni2p<sub>3/2</sub>, Zn2p<sub>3/2</sub>, O 1s and C 1s were acquired at the analyser pass energy of 20 eV with 0.1 eV steps. Vacuum in the analysing chamber was kept at 1.33 10<sup>-7</sup> Pa. The empirical sensitivity factors for these elements were taken from reference [17] and the spectra obtained were compared with the standard ones [18]. All Ar<sup>+</sup> sputtering was performed at 2.0 and 4.0 kV operating in vacuum of 5 10<sup>-3</sup> Pa. This corresponds to an etching rate of ~2 nm min<sup>-1</sup>. The duration of etching was 60, 180, 480, and 930 s. The maximum accuracy of the method was ± 0.1 at.%.

## RESULTS AND DISCUSSION

### 1. Identification of optimal potentiodynamic stripping conditions

To obtain a precise phase composition of Zn–Ni alloys it is necessary to choose the optimum thick-

ness of deposits and a suitable potential sweep rate (*v*). Data in Fig. 1 (a) show that even potentiodynamic stripping data of a very thin layer of Zn–Ni alloys (~0.035 μm) deposited at *i<sub>c</sub>* = 0.006 A cm<sup>-2</sup>, τ = 15s are distorted with an increase in *v* up to 0.050 V s<sup>-1</sup>, because the alloy dissolution which as was expected should be completed in the negative potential range at *E* < 0.0 V, actually was shifted towards positive potentials at higher values of potential sweep rate.

With an increase in the deposition time at *i<sub>c</sub>* = 0.006 A cm<sup>-2</sup> from 15 s to 150 s (Fig. 2 (a)) the potentiodynamic stripping response of Zn–Ni alloy at

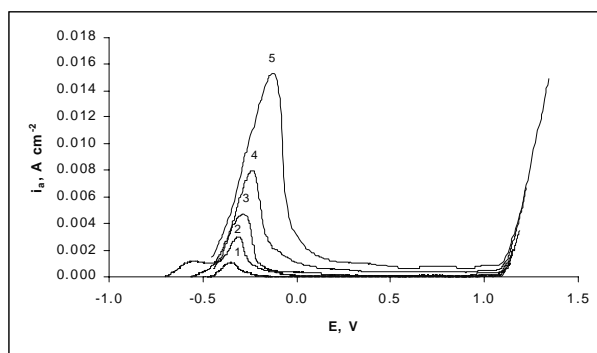


**Fig. 1.** Potentiodynamic stripping response of Zn–Ni coatings deposited in nickel plating solution containing 0.227 mol l<sup>-1</sup> of ZnCl<sub>2</sub> at (*i<sub>c</sub>* = 0.006 A cm<sup>-2</sup>, τ = 15 s, *t* = 50 °C) versus potential sweeping rate (*v*) (V s<sup>-1</sup>): (1) 0.005; (2) 0.010; (3) 0.020; (4) 0.050; (5) 0.100

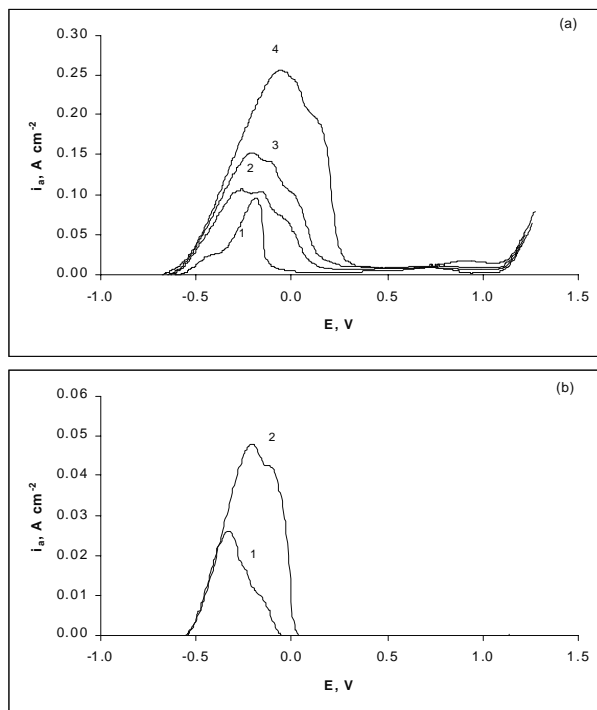


**Fig. 2.** Potentiodynamic stripping response of Zn–Ni coatings deposited in nickel plating solution containing 0.227 mol l<sup>-1</sup> of ZnCl<sub>2</sub> at (*i<sub>c</sub>* = 0.006 A cm<sup>-2</sup>, τ = 15 s, *t* = 50 °C) versus deposition time (*s*): (a) *v* = 0.020 V s<sup>-1</sup> (1) 30; (2) 60; (3) 90; (4) 150. (b) *v* = 0.005 V s<sup>-1</sup> (1) 300; (2) 660

$v = 0.020 \text{ V s}^{-1}$  was similar to that at  $v = 0.100 \text{ V s}^{-1}$  (Fig. 1). The potentiodynamic stripping  $i_a$  peaks are shifted towards more positive potentials up to 0.25 V with an increase in deposition time and the stripping data are distorted. When the potential sweep rate is decreased to  $0.005 \text{ V s}^{-1}$  alloys are dissolved completely at  $E < 0.0 \text{ V}$  even with an increase in the deposition time up to 660 s (Fig. 2 (b)). Therefore, it is advisable to use  $v \leq 0.005 \text{ V s}^{-1}$  and coating thickness  $\leq 6 \mu\text{m}$  as working conditions.

## 2. Dependence of variations in the phase composition of Zn–Ni alloy on deposition conditions

### 2.1 Influence of temperature

An anomalous Zn–Ni codepositon occurs when the concentration of  $[\text{Ni}^{+2}]$  in the electrolyte is high and a great quantity of Zn is present in the alloy. At  $20^\circ\text{C}$  an anomalous Zn–Ni codeposition begins, while the  $[\text{Zn}^{+2}] / [\text{Ni}^{+2}]$  ratio in acetate-chloride electrolyte is higher than 0.02 and the Zn / Ni ratio in alloy is higher than 2 [4]. The potentiodynamic stripping curves (PDC) of Zn–Ni alloys deposited under anomalous conditions exhibit  $i_a$  peaks only at  $E < 0.0 \text{ V}$ , which evidences that pure Ni which could be anodically dissolved at  $E > 0.0 \text{ V}$  in the  $i_a$  peak H is absent in the alloy [4]. Potentiodynamic stripping data of the Zn–Ni alloys deposited at various temperatures are presented in Fig. 3. The  $i_a$  peaks which correspond to dissolution of the Zn–Ni alloy only at  $E < 0.0 \text{ V}$  emerge in the stripping PDC of Zn–Ni alloys deposited at temperatures of  $20^\circ\text{C}$  and  $30^\circ\text{C}$ . These  $i_a$  peaks are resultants of the  $i_a$  peaks B, C and D. The resultants correspond to dissolution of Zn from  $\alpha$ - and  $\gamma$ -phases, respectively; the  $i_a$  peak A which corresponds to dissolution of Zn from  $\eta$ -phase is not observed in PDCs. When the deposition temperature of Zn–Ni alloy is increased up to  $40^\circ\text{C}$ , the  $i_a$  peak H arises in the PDC at  $E > 0.0 \text{ V}$ , implying that pure Ni is absent in the coating. The  $i_a$  peak H, which is conditioned by an increase in Ni quantity in the alloy, prevails in the stripping PDCs when the deposition temperature is increased up to  $50^\circ\text{C}$ .

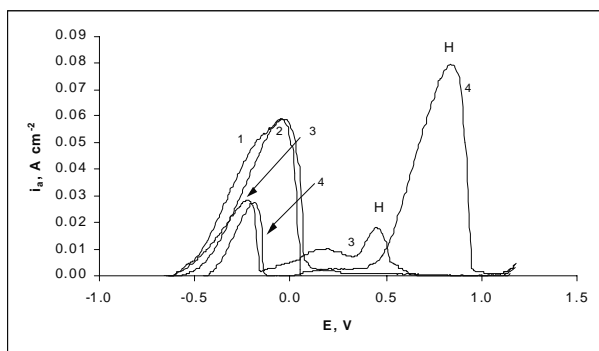


**Fig. 3.** Potentiodynamic stripping ( $v = 0.005 \text{ V s}^{-1}$ ) response of Zn–Ni coatings deposited in nickel plating solution containing  $0.030 \text{ mol l}^{-1}$  of  $\text{ZnCl}_2$  at ( $i_c = 0.006 \text{ A cm}^{-2}$ ,  $\tau = 1320 \text{ s}$ ), versus deposition temperature ( $^\circ\text{C}$ ): (1) 20; (2) 30; (3) 40; (4) 50

### 2.2 Influence of Zn–Ni alloy thickness

According to Ref. [8], when the  $[\text{Zn}^{+2}] / [\text{Ni}^{+2}]$  ratio in plating solution is constant, the Zn / Ni ratio in the alloy depends on the thickness of coating. Therefore, the stripping studies of the coatings deposited at  $i_c = 0.006 \text{ A cm}^{-2}$  with an increase in both the deposition time from 15 s to 2640 s and the thickness from  $0.035 \mu\text{m}$  to  $5.2 \mu\text{m}$ , respectively, were performed in the present work. Under potentiodynamic stripping of Zn–Ni alloy deposited in a plating solution containing  $0.030 \text{ mol l}^{-1} \text{ ZnCl}_2$  at  $50^\circ\text{C}$  (Fig. 4) it has been determined that when the thickness of coatings varies from  $0.035 \mu\text{m}$  to  $0.6 \mu\text{m}$  the  $i_a$  peaks prevail in the stripping PDC at  $E < 0.0 \text{ V}$ , while small  $i_a$  peaks H emerge at  $E > 0.0 \text{ V}$ . When the thickness of coating is increased from  $1.32 \mu\text{m}$  to  $2.64 \mu\text{m}$ , the  $i_a$  peaks H which emerge at  $E > 0.0 \text{ V}$  prevail in the stripping PDC.

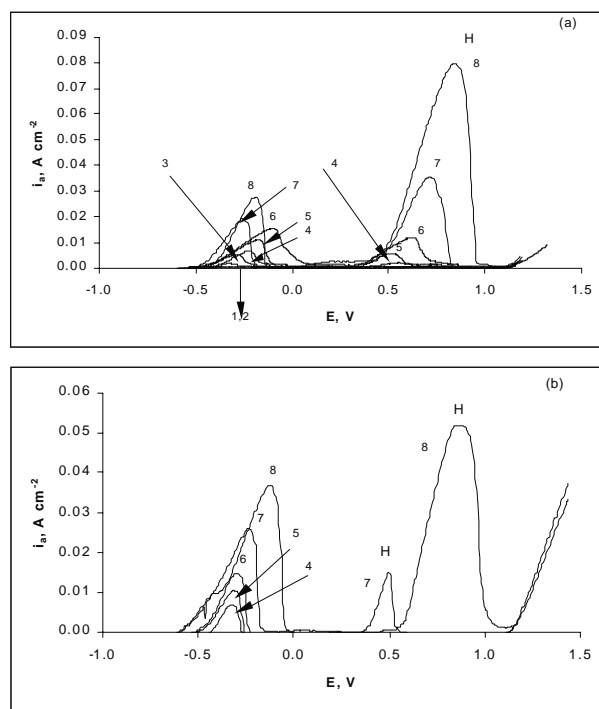


**Fig. 4.** Potentiodynamic stripping ( $v = 0.005 \text{ V s}^{-1}$ ) response of Zn–Ni coatings deposited in nickel plating solution containing (a)  $0.030 \text{ mol l}^{-1}$  and (b)  $0.114 \text{ mol l}^{-1}$  of  $\text{ZnCl}_2$  at ( $i_c = 0.006 \text{ A cm}^{-2}$ ,  $t = 50^\circ\text{C}$ ) versus deposition time (s): (1) 15; (2) 30; (3) 60; (4) 90; (5) 150; (6) 300; (7) 660; (8) 1320

Analysis of Zn–Ni alloys of various thickness showed that the Zn / Ni ratio in the alloy varied very slightly with an eightfold increase in the thickness of coating (Table 1). Moreover, very small variations in the Zn / Ni ratio in the alloy were determined during analysis of both sides of the coating, whereas the composition of the  $\alpha$ -phase is not constant and analysis confirmed that variations in Ni quantity in the alloy were only slight, so it was possible to make an assumption that when the compo-

**Table 1. Total  $CE_t$  of Zn–Ni alloy and partial  $CE$  of Zn–Ni alloys that can dissolve at  $E < 0.0$  V ( $CE_1$ , %) and at  $E > 0.0$  V ( $CE_2$ , %) in  $i_a$  peak H depending on temperature ( $t$ , °C) and deposition time ( $\tau$ , s). Coatings were deposited in plating solution containing  $0.030 \text{ mol l}^{-1}$  of  $\text{ZnCl}_2$  at  $i_c = 0.006 \text{ A cm}^{-2}$**

$\tau$ , s		15	30	60	90	150	300	660	1320
20 °C	$CE_t$ , %	26.6	35.5	43.3	43.2	47.1	49.2	49.8	52.7
50 °C	$CE_t$ , %	39.4	69.8	71.7	78.6	79.7	81.7	71.2	56.1
	$CE_1$ , %	21.5	39.2	51.4	44.6	49.9	43.4	18.5	8.4
	$CE_2$ , %	17.9	30.6	20.3	34.0	29.8	38.3	52.7	47.7

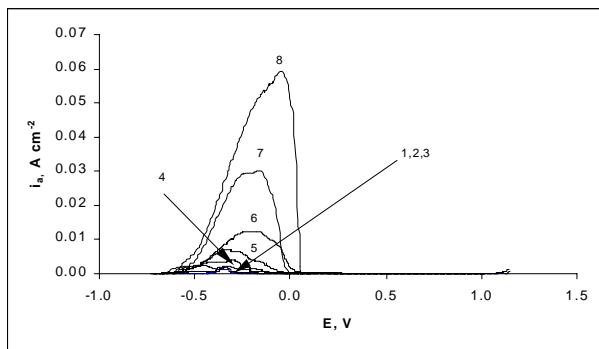


**Fig. 5.** Potentiodynamic stripping ( $v = 0.005 \text{ V s}^{-1}$ ) response of Zn–Ni coatings deposited in nickel plating solution containing (a)  $0.030 \text{ mol l}^{-1}$  of  $\text{ZnCl}_2$  at ( $i_c = 0.006 \text{ A cm}^{-2}$ ,  $t = 20$  °C) versus deposition time (s): (1) 15; (2) 30; (3) 60; (4) 90; (5) 150; (6) 300; (7) 660; (8) 1320

sition of the  $\alpha$ -phase undergoes changes, the Ni quantity in this phase decreases and therefore a certain proportion of Ni is deposited in the form other than the Zn–Ni alloy.

Data similar to those presented above were obtained under potentiodynamic stripping of coatings deposited in a plating solution containing  $0.114 \text{ mol l}^{-1}$   $\text{ZnCl}_2$  at  $50$  °C (Fig. 5). In this case redistribution of Zn–Ni alloy phases began at a thickness of coatings  $2.5 \mu\text{m}$  and more.

Under potentiodynamic stripping of the Zn–Ni alloy deposited in an electrolyte containing  $0.030 \text{ mol l}^{-1}$   $\text{ZnCl}_2$  at  $20$  °C the phase variations in the alloy were not observed and the whole alloy was dissolved at  $E < 0.0$  V (Fig. 6). The case mentioned above indicates that pure Ni is absent in the coating.

On the basis of the potentiodynamic stripping data presented above the current efficiency ( $CE$ ) and the distribution of the phases that are potentiodynamically dissolved at  $E < 0.0$  V ( $CE_1$ ) and at  $E > 0.0$  V ( $CE_2$ ) in the alloy depending on the coating thickness and deposition temperature were calculated (Table 1). It was determined that dissolution of Zn–Ni alloy deposited at  $20$  °C occurred at  $E < 0.0$  V irrespective of coating thickness. With an increase in the thickness of Zn–Ni alloy the  $CE_t$  increased with an increase in the deposition time up to  $150$  s. With the further increase in thickness

of alloy,  $CE_t$  was approximately equal to  $50\%$ . More complex processes occurred while Zn–Ni alloy was deposited at  $50$  °C. When the deposition time of Zn–Ni alloy was increased up to  $300$  s,  $CE_t$  reached  $80\%$  and a clear distribution of phases in the alloy was not observed. With an increase in deposition time up to

$1320$  s,  $CE_t$  began to decrease to  $56\%$ . This decrease was accompanied by a redistribution of phases in the Zn–Ni alloy. When the deposition time was increased from  $300$  s to  $1320$  s, Zn–Ni alloy contained approximately of  $8.4$  weight% of the phase that dissolved at  $E < 0.0$  V.

### 2.3 Influence of $i_c$

With an increase in the concentration of  $\text{ZnCl}_2$  in the plating solution from  $0.030 \text{ mol l}^{-1}$  to  $0.114 \text{ mol l}^{-1}$ , the  $CE$  of Zn–Ni alloy deposited at  $50$  °C passes through a minimum when the plating solution contains from  $0.059 \text{ mol l}^{-1}$  to  $0.076 \text{ mol l}^{-1}$   $\text{ZnCl}_2$ . [4] It means that normal Zn–Ni codeposition becomes anomalous. Therefore, the studies of the phase composition of the alloys deposited in the electrolyte containing from  $0.030 \text{ mol l}^{-1}$   $0.114 \text{ mol l}^{-1}$   $\text{ZnCl}_2$  at various  $i_c$  were performed.

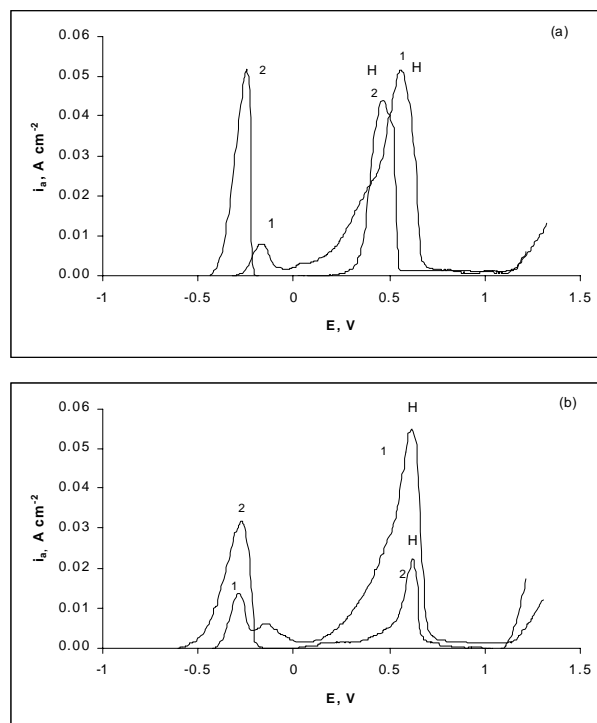


**Fig. 6.** Potentiodynamic stripping ( $v = 0.005 \text{ V s}^{-1}$ ) response of Zn–Ni coatings deposited in nickel plating solution containing (a)  $0.030 \text{ mol l}^{-1}$  (b)  $0.059 \text{ mol l}^{-1}$  (c)  $0.114 \text{ mol l}^{-1}$  of  $\text{ZnCl}_2$  at ( $i_c = 0.006 \text{ A cm}^{-2}$ ,  $t = 20$  °C) versus  $i_c$  ( $\text{A cm}^{-2}$ ): (1)  $0.002$  (2)  $0.005$

Table 2. Dependence of Ni quantity (wt.%) on  $i_c$  and  $\text{ZnCl}_2$  concentration in electrolyte.  $t = 50^\circ\text{C}$

$c$ , mol l <sup>-1</sup>	Ni, wt. %	
	$i_c$ , A cm <sup>-2</sup>	
	0.002	0.005
0.030	87.7	82.9
0.059	76.4	76.7
0.114	82.0	42.2

Table 3. Total  $CE_t$  (%) of Zn–Ni alloy deposition and partial  $CE$  of Zn–Ni alloys that can dissolve at  $E < 0.0$  V ( $CE_1$ , %) and at  $E > 0.0$  V ( $CE_2$ , %)  $i_a$  peak H,  $CE_{tw}$  (%) determined by gravimetric method and  $\Delta = CE_{tw} - CE_t$  (%) depending on  $\text{ZnCl}_2$  concentration in plating solution ( $c$ , mol l<sup>-1</sup>) and  $i_c$  (A cm<sup>-2</sup>).  $t = 50^\circ\text{C}$

$c$ , mol l <sup>-1</sup>	0.002 A cm <sup>-2</sup>			0.005 A cm <sup>-2</sup>				
	$CE_t$	$CE_1$	$CE_2$	$CE_t$	$CE_1$	$CE_2$	$CE_{tw}$	$\Delta$
0.030	81.7	6.0	75.7	65.1	27.5	37.2	79.9	14.8
0.059	83.0	12.9	70.1	46.4	28.7	17.7	66.3	19.9
0.114	65.0	31.0	34.0	61.0	24.2	36.8	68.1	7.1

It was determined that with an increase in  $i_c$  the quantity of Zn–Ni alloy dissolved at  $E < 0.0$  V increased, while the quantity of Ni dissolved in the vicinity of the  $i_a$  peak H increased with a decrease in  $i_c$  (Fig. 6). Inasmuch as the potentiodynamic stripping of  $i_a$  peaks shows a dissolution of Zn from certain phases of Zn–Ni alloy, which was confirmed by XRD studies [7–9, 11, 13], it may be supposed that the insignificant variations in the Ni quantity in alloy cause (Table 2) some substantial variations in the phase composition of the alloy (Fig. 6, curves 1 and 2). It suggests that both the Zn / Ni ratio in the alloy and  $i_c$  affect the phase composition of Zn–Ni alloy.

On the basis of the potentiodynamic stripping data presented above, the total current efficiency ( $CE$ ) and the partial current efficiencies of the phases that are potentiodynamically dissolved at  $E < 0.0$  V ( $CE_1$ ) and at  $E > 0.0$  V ( $CE_2$ ) in the alloy depending on  $\text{ZnCl}_2$  concentration in the plating solution and  $i_c$  were calculated (Table 3). While  $CE_t$  of the coatings deposited at  $i_c = 0.002$  A cm<sup>-2</sup> decreased, the  $CE_1$  increased with an increase in  $\text{ZnCl}_2$  concentration in the plating solution. The  $CE_t$  of the coatings deposited at  $i_c = 0.005$  A cm<sup>-2</sup> passed through a minimum, while  $CE_1$  passed through a maximum. It shows a clear correlation between  $CE_t$  and  $CE_1$ .

A comparison of the data obtained by the potentiodynamic stripping method and those obtained by the gravimetric method showed that  $CE_t$  obtained by the gravimetric method was higher than that obtained by the potentiodynamic method. The difference in data showed that high quantities of oxides and hydroxides were present in the coatings deposited at  $50^\circ\text{C}$ . The quantities of oxides and hydroxides decreased with an increase in  $[\text{Zn}^{+2}]$  in the plating solution. These data were confirmed by the XPS method. From in-depth profiles one can see that both sides of Zn–Ni alloy were oxidized with various oxygen content: the first point at 0 s of sputtering times indicated that the surface of Zn–Ni coating (Table 4) was covered with less oxide compounds than the other side from the Ti substrate. When the depth profile went to 108 s, the O concentration decreased from Ti substrate considerably quicker, and it contained 8.5 at.% O while the coating surface contained 28.8 at.% O.

Table 4. Depth profiling results of oxygen (at.%) in Zn–Ni alloy deposited in acetate-chloride electrolyte containing 0.227 mol l<sup>-1</sup>  $\text{ZnCl}_2$  at  $20^\circ\text{C}$   $i_c = 0.010$  A cm<sup>-2</sup>,  $\tau = 5400$  s (01) after etching by argon-ion from the surface of coating and (02) from the side of Ti substrate

Table 4. Depth profiling results of oxygen (at.%) in Zn–Ni alloy deposited in acetate-chloride electrolyte containing 0.227 mol l<sup>-1</sup>  $\text{ZnCl}_2$  at  $20^\circ\text{C}$   $i_c = 0.010$  A cm<sup>-2</sup>,  $\tau = 5400$  s (01) after etching by argon-ion from the surface of coating and (02) from the side of Ti substrate

Etching time, s	0	12	48	108	198
Data from coating surface	35.6	46.0	44.8	28.8	17.1
Data from the side of Ti substrate	39.1	38.1	26.5	8.5	–

A visual inspection of Zn–Ni coating showed that Zn–Ni alloys became lighter with an increase in  $[\text{Zn}^{+2}]$  in plating solution, implying that the black colour of Zn–Ni alloy depended on the quantity of oxides and hydroxides in the alloy.

## CONCLUSIONS

1. The quantity of free Ni in the Zn–Ni alloy increases with an increase in the temperature of acetate–chloride electrolyte.
2. The phase composition of Zn–Ni alloy deposited at  $50^\circ\text{C}$  depends on the thickness of the coating and  $i_c$ . The quantity of free Ni in the alloy increases with a decrease in  $i_c$  or an increase in alloy thickness.

Received 9 November 2004  
Accepted 24 November 2004

## References

1. D. E. Hall, *Plat. and Surf. Fin.*, **70** (11), 59 (1983).
2. F. J. Fabri Miranda, O. E. Barcia, S. L. Diaz, O. R. Mattos and R. Wiart, *Eletochim Acta*, **41** (7-8), 1041 (1996).
3. F. Elkhatibi, M. Benballa, M. Sarret and C. Müller, *Electrochim. Acta*, **44** (10), 1645 (1999).
4. A. Petrauskas, L. Grinceviënė, A. Ėesūnienė and E. Matulionis, *Surf. Coat Technol.* (in press).
5. J. Garcia, J. Barcelo, M. Sarret, C. Müller and J. Pregonas, *J. Appl. Electrochem.*, **24**, 1249 (1994).

6. M. Gavrilă, J. P. Millet, H. Mazille, D. Marchandise and J. M. Cuntz, *Surf. Coat Technol.*, **123**, 164 (2000).
7. S. Swathijaran, *J. Electrochem. Soc.*, **133** (4), 671 (1986).
8. F. Elkhatabi, M. Sarret and C. Müller, *J. Electroanal. Chem.*, **404** (1), 45 (1996).
9. C. Müller, M. Sarret and M. Benballa, *Electrochim. Acta*, **46** (18), 2811 (2001).
10. J. Stevanovic, S. Gojkovic, A. Despic, M. Obradovic and V. Nakic, *Electrochim. Acta*, **43** (7), 705 (1998).
11. F. Elkhatabi, G. Barcelo, M. Sarret and C. Muller, *J. Electronal. Chem.*, **419** (1), 71 (1996).
12. Yo-Po Lin and R. Selman, *J. Electrochem. Soc.*, **140** (5), 1299 (1993).
13. A. Petrauskas, L. Grincevièienė, A. Èeðûnienė and R. Juðkėnas, *Electrochim. Acta* (article in press).
14. E. Beltowska-Lehman, P. Ozga, Z. Swaitek and C. Lupi, *Surf. Coat. Technol.*, **151-152**, 444 (2002).
15. A. Petrauskas, L. Grincevièienė, A. Èeðûnienė and M. Kurtinaitienė, *Cheminė technologija* (article in press).
16. S. S. Abd El Rehim, E. E. Foad, S. M. Abd El Wahab and Hamdy H. Hassan, *Electrochim Acta*, **41** (9), 1413 (1996).
17. Анализ поверхности методом оже- и рентгеновской фотоэлектронной спектроскопии / под ред. Д. Бриггса и М. П. Стиха, Москва. С. 598 (1987).
18. C. D. Wagner, W. M. Riggs, L. E. Davis and J. F. Moulder et al., *Handbook of X-ray Photoelectron Spectroscopy*. Perkin-Elmer Corporation. Minnesota (1978).

**A. Petrauskas, L. Grincevièienė, A. Èeðûnienė, V. Jasulaitienė**

**ZN-NI SÀSÈDPIO ACETATINIAME-CHLORIDINIAME ELEKTROLITE PRIKLAUSOMYBÈS NUO NUSODINIMO SÀLYGØ TYRIMAS**

**S a n t r a u k a**

Darbe iðtirta Zn ir Ni sàsėdpio acetatiniame-chloridiniame elektrolite priklausomybė nuo katodinės srovės tankio, nusodinimo elektrolito temperatūros ir sluoksnio storio potenciodinaminio stripingo metodu. Nustatyta, kad didinant nusodinimo elektrolito temperatūrą didėja laisvo Ni kiekis dangose. 50°C temperatūros elektrolite maþinant nusodinimo  $i_k$  tokio pat storio sluoksnio dangose didėja laisvo Ni kiekis. Didinant nusodinamø dangø sluoksnio storá kinta jø fazinė sudėtis.